FEATURE EXTRACTION AND CHANGE DETECTION FOR BRIDGES OVER WATER IN AIRBORNE AND SPACEBORNE SAR IMAGE DATA

Erich Cadario[1], Karsten Schulz[1], Hermann Gross[1], Horst Hammer[1], Antje Thiele[1], Ulrich Thoennessen[1], Dan Johan Weydahl[2] and Uwe Soergel[3]

1. Research Institute for Optronics and Pattern Recognition (FOM), Ettlingen, Germany; cadario@fom.fgan.de
2. Norwegian Defence Research Establishment (FFI), Land and Airsystems Division, Kjeller , Norway; Dan-Johan.Weydahl@ffi.no
3. Leibniz Universität Hannover, Institute of Photogrammetry and GeoInformation (IPI), Hannover, Germany; soergel@ipi.uni-hannover.de

ABSTRACT

Key elements of man-made infrastructure are bridges. In case of natural disasters, it is important to get real-time information about these objects. Such up-to-date information-requirements can be fulfilled by Synthetic Aperture Radar sensors. The main advantage of SAR is the availability of data under nearly all weather conditions and at any day time. Especially in the case of bridges over water, the SAR specific side looking imaging geometry can lead to special characteristics in the image. A bridge can appear as several bright stripes in the SAR image if certain prerequisites are fulfilled. These stripes can be segmented, and some bridge features like width and height can be derived.

In this paper, the possibilities to extract features like width and height from the mentioned stripes are discussed. An approach is presented to segment these stripes in SAR or InSAR data and to exploit this special signature for change detection. The investigations are supported by simulations based on a ray tracing approach. Aim of the simulations is an assessment of acceptable imaging constellations for a certain bridge. Here acceptable means constellations, where the special signature can be expected. Real data examples for high-resolution airborne (resolution better than 40 cm) and spaceborne (RADARSAT-1, approx. 9 m resolution) sensors are presented. The results show that a feature like bridge height can successfully be derived from SAR data by using a description of the bridge on an object level. A concept is proposed to use this description for change detection by integration in a GIS-system.

INTRODUCTION

Optical image acquisition for disaster management is hampered by its weather and time-of-day dependency. SAR (Synthetic Aperture Radar) by contrast is a remote sensing technique capable to deliver actual data at any time and under bad weather conditions. Before launch of TerraSAR-X (i), RADARSAT-2 (ii), and COSMO-SkyMed (iii), the rather coarse resolution of operational SAR satellite systems allowed an analysis of spaceborne SAR data in case of disaster management only for medium scale products, for example generation of change masks after volcano eruptions (iv), earthquakes (v) or flood maps (vi). The new generation of spaceborne SAR satellites allows a more detailed analysis at the object level, which was before restricted to airborne SAR sensors (vii). Modern airborne SAR sensors deliver actually resolutions in the decimetre scale, which leads to new challenges in image interpretation and analysis (viii). Data of that kind were already investigated for example in the context of road extraction (ix) and building recognition (x), (xi) in urban scenes.

Bridges are key-elements of man-made infrastructure. They connect traffic networks and therefore it is vital to get real-time information about these objects for example to assess the possibilities of delivering food to affected people in case of natural disasters. The detection of bridges in high-

ISBN 978-3-925143-79-3

resolution SAR data was for example investigated in (xii) and (xiii). For bridges over water, different types of scattering events may result in the appearance of several bridge images at separated range locations (xiv), (xv), (xvi). This depends on viewing conditions and the kind of illuminated object (concerning e.g. aspect, depression angle, and material). The main scattering events responsible for this signature are: direct backscatter, double-bounce reflection between water surface and the side of the bridge structure facing the sensor, and triple-bounce reflection involving bottom side of the bridge deck and water surface. If PolSAR (Polarimetric SAR) data are available, even and odd numbers of scattering events can be distinguished (xvii). The location of the described effects is predictable from the given SAR viewing geometry and the bridge's structure and the corresponding bright stripes in the SAR image can be exploited to extract features like width and height.

Change detection in SAR images is an important field of research. In (xviii) the focus was especially on changes of small bridges; the signature of small bridges before and after a damage was simulated. There the focus of analysis was on a pixel level. In this paper, the signature of bridges over water in SAR data is discussed and an approach for change detection is presented, exploiting predictable effects on an object level: in a first step, information about significant features of a specific bridge have to be derived from a reference image and stored in a database together with the imaging parameters and additionally the parameters which were used for automatic feature extraction. These parameters are afterwards used to extract these features from other images of the same object if the imaging constellation fulfils predicted requirements. If the requirements are fulfilled, but the features were not extracted, a change is supposed. The assessment of imaging constellations which will allow a successful extraction is supported by simulations. In the first section, examples of the appearance of bridges over water in spaceborne (RADARSAT-1, approx. 9 m resolution) and high-resolution airborne (resolution better than 40 cm) SAR and InSAR data are shown and geometric constraints concerning the appearance of bridge signature are discussed. In the next sections, change detection approach and simulations for a simple bridge model are presented and finally results are shown and the paper is concluded.

BRIDGES OVER WATER IN SAR DATA

Bridges over water illuminated orthogonal to their orientation may cause multiple images in SAR data. Usually three parallel stripes are observed at increasing range locations (Figure 1): first direct backscatter from the bridge, followed by double-bounce reflection between bridge and water or vice versa, and finally triple reflection (water, lower parts of the bridge and water again).

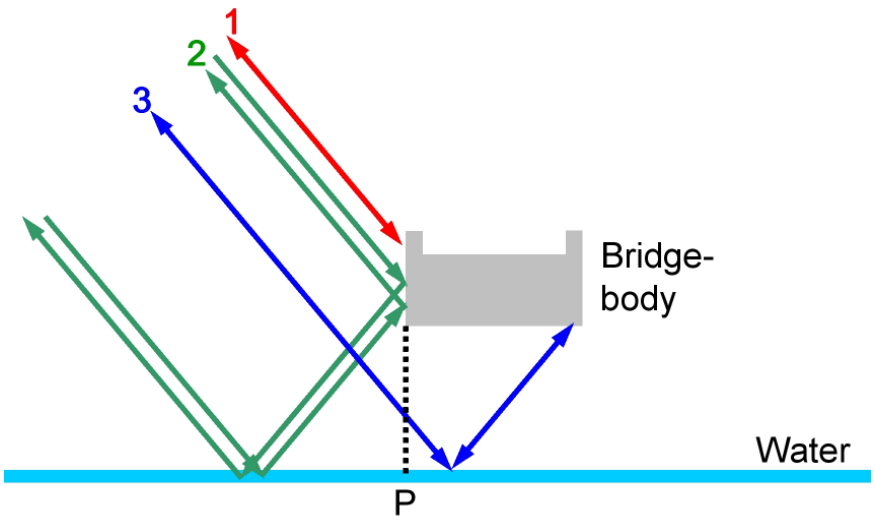

Figure 1: Model for bridge over water and corresponding three stripes in a SAR image.

ISBN 978-3-925143-79-3

Often superstructure elements and piles are also visible. This was already shown in the literature for SAR satellite magnitude imagery (xv). Additionally multi-bounce signal of lower magnitude eventually may show-up at even larger ranges caused by pairs of back and forth bouncing between the bridge's lower side and the water (xvii). An example for a spaceborne SAR image (RADARSAT-1, resolution approx. 9 m) is shown in Figure 2.

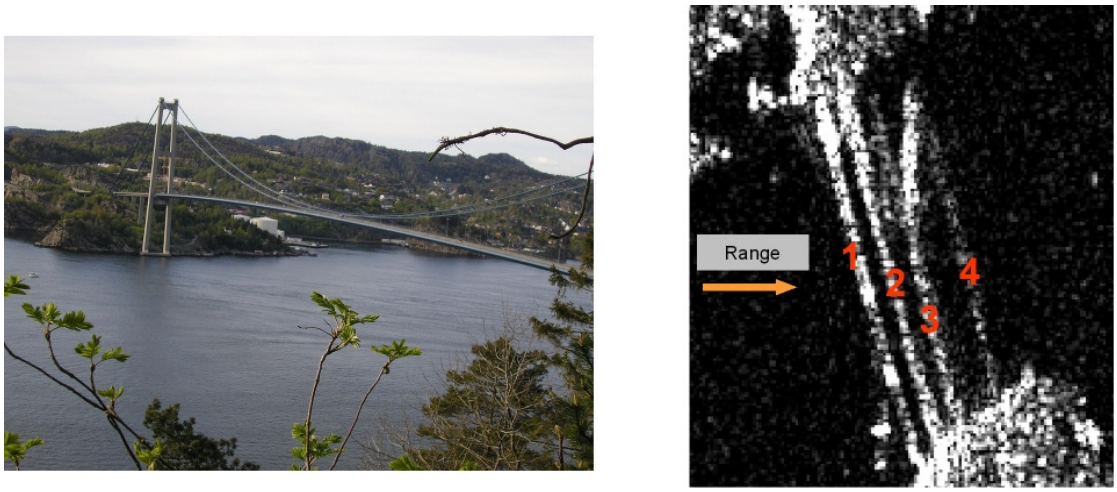

Figure 2: Photo of a suspension bridge in Norway(left) and RADARSAT-1 signature of this bridge (right).

Direct reflection from the bridge deck is denoted with 1. According to the construction principle of a suspension bridge, signal from the cables and from the bridge deck overlap in the middle of 1. The stripe marked with 2 results from two contributions: double-bounce reflection between water surface and side of the bridge (path: sensor – water – bridge – sensor or vice-versa) and additionally from double-bounce signal between water and cables. Due to the fact, that the ocean surface is flat, the roundtrip time in these cases corresponds to points vertically projected on the ocean surface, independently from the height of the points (this situation is comparable to dihedral corner reflectors between a building wall and the ground, resulting in the so called corner-lines (xi)). The signal labelled with 3 is caused by triple-bounce reflections (path: sensor – water – bridge deck bottom side – water – sensor; path: sensor – water – cable – water – sensor). According to the investigations in (xvii), the signal denoted with 4 can be probably ascribed to higher order multiple bounces (path: sensor – water – bottom of bridge deck – water – bottom of bridge deck – water – sensor).

In Figure 3, an example for a small bridge in high resolution airborne InSAR data is shown. This data was recorded in X-band with the AeS-1 sensor of Intermap company (xix) with a resolution of approx. 40 cm.

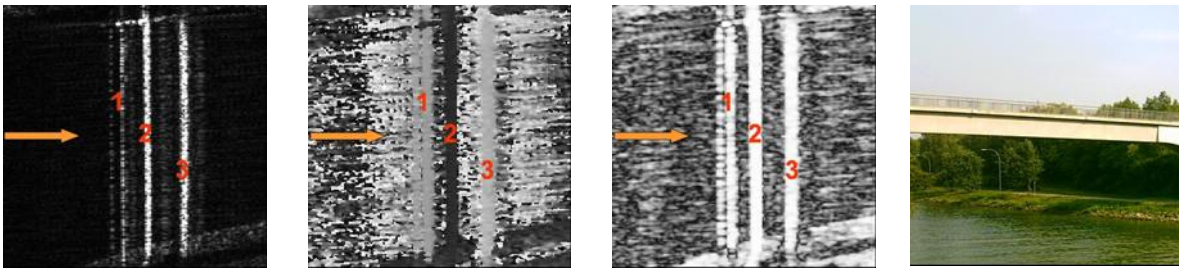

a b c d

Figure 3: Small bridge in high resolution airborne InSAR data, illumination direction from left. magnitude (a), interferometric phase (b), coherence (c), photo (d)

ISBN 978-3-925143-79-3

Direct reflection from the bridge deck is again denoted with 1, double-bounce reflection with 2 and triple-bounce reflection with 3. Due to the high resolution, even the railing is observable as dotted line at closest distance to the sensor.

The distance of these stripes can be exploited to extract bridge features like height and width from a SAR image. Additionally the interferometric phase can be used to derive the bridge height (xx). In this paper the focus is on geometric relations between the first to stripes to derive the bridge height h, which can be calculated according to (xvi) (xx) by: h = (s2-s1) / cos(theta), where theta is the incidence angle, and (s2-s1) is the slant-range distance between the second stripe (caused by double-bounce reflection) and the border of the layover area (caused by direct reflection). To calculate the height, the first two stripes have to be segmented in an image, and these stripes and the corresponding height respectively, are the features that will be used in the change detection approach that is described in the next section.

CHANGE DETECTION APPROACH

Afore mentioned stripes are the base for a change detection approach for bridges over water. The whole process is depicted in Figure 4. In case of disaster management, the question to answer is not 'where is a bridge', but 'is a certain bridge affected'. So, a priori knowledge about the geolocation of a bridge is assumed to be achievable. The process starts with the extraction of the feature ‘parallel lines’ and the corresponding height respectively from a reference image. The extracted features are stored in a database, together with the algorithm parameters that were used for the extraction. The algorithm parameters can be optimized by a human operator because this initial step is not time critical.

ISBN 978-3-925143-79-3

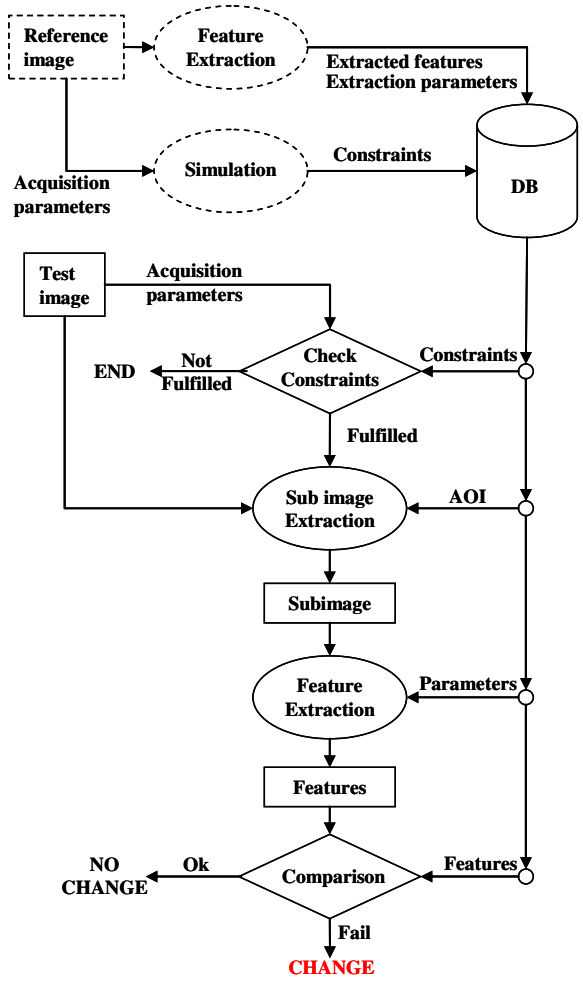

Figure 4: Flow chart of change detection approach.

Additionally simulations are performed to derive constraints concerning the imaging constellations that are suitable for the extraction of these features for the given object (e.g. modifying aspect, incidence angle). For a new image, first the imaging constellation is compared with the appropriate configurations. If the constraints are fulfilled, an AOI (area of interest) is calculated for the object under investigation and a new sub image is created. Here it is supposed, that the coordinates of a bridge object are known and that the georeferencing accuracy of the image is precise enough (this can be assumed for all modern spaceborne and airborne sensors). The stored parameters for feature extraction are used also for the new image to look for the 'parallel lines'. If the searched feature is found, no change is reported, otherwise a change is indicated.

The segmentation step works as follows. The segmentation starts with generation of a corresponding sub image from logarithmic scaled data, including knowledge about the position accuracy of the dataset under investigation. After it, a segmentation of curvilinear structures using Steger-operator (xxi) is performed in this sub image. These structures are fitted to straight lines in a subsequent step. A priori knowledge about the expected bridge dimensions is coded into a bridge model and the detected lines are filtered regarding their length. The remaining ones are grouped to pairs or triplets of parallel lines and, if necessary, once more filtered based on their distance. The corresponding filter parameter is derived from the bridge model and the expected bright line distances. To derive the height, the middle of the stripes is used here. An example for the described segmentation in RADARSAT-1 data is presented in Figure 5.

ISBN 978-3-925143-79-3

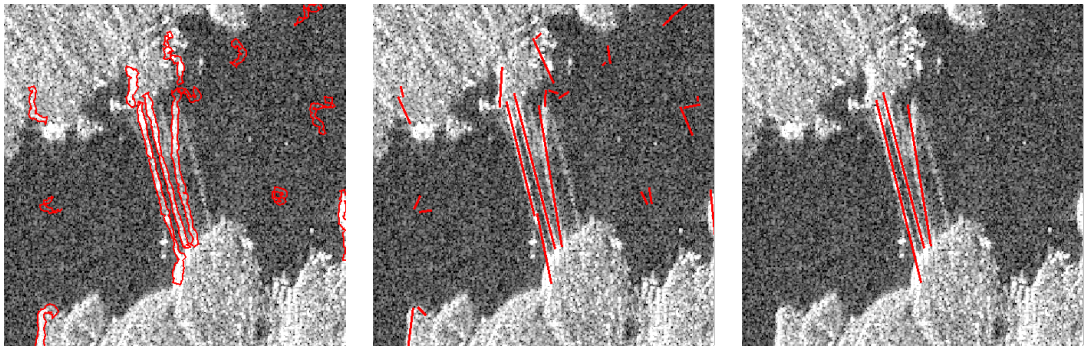

a b c

Figure 5: Detection of parallel lines in RADARSAT-1 data. Result of: Steger-operator (a), Line Fitting (b), Filter (c). Illumination always from left.

The result of the Steger-operator is shown in (a); line fitting- and filter result are illustrated in (b) and (c), respectively. In this case, filtering based on the length alone delivers good results. Three lines were detected, whereas the one derived from triple-bounce reflection signature is slightly 'unparallel'. Signal caused by triple-bounce reflection from the cables has in the upper part main influence on the detection result.

SIMULATION

One goal of this investigation is to predict if the above introduced geometric feature 'parallel lines' can be expected for a given imaging constellation. For this purpose simulations of radar backscatter were performed with different incidence angle and material parameters. The results shown here represent just the beginning of these investigations. The new simulation-tool will be further developed in the future to deliver more detailed backscatter results for different materials and complex objects like suspension bridges. Here the focus is on more simple bridge models.

Input data for the simulator consist of a file containing a CAD-model of the scene to be rendered. From this, a 3D-model of the scene is created. The simulation tool is based on narrow beam approximation of the radar signal. This means that the (wide) RADAR-beam sent by the emitter is approximated by a narrow beam. This allows the use of ray tracing techniques in the calculation of the simulated SAR image. In fact, the narrow beam simulated image is quite a good approximation of what one gets after the processing of (wide beam) SAR raw data. Since the narrow beam technique opens the opportunity to model the phase, a complex image is generated, i.e. returns from the same voxel are added coherently. Several materials are modelled considering their most relevant physical properties, such as reflectivity for the RADAR signal. The user can specify the number of specular reflections to be calculated. After each specular reflection a physical optics (PO) scattering return is calculated. The energy reflected back to the receiver by PO is also weighted by a discrete Ulaby-model of the material used (xxii) and is thus dependent on the incidence angle. Finally, to render the image more realistic, a user-specified amount of point scatterers is randomly placed in each voxel and the returns of these point scatterers are coherently added to get the final intensity signal to the receiver by this voxel.

ISBN 978-3-925143-79-3

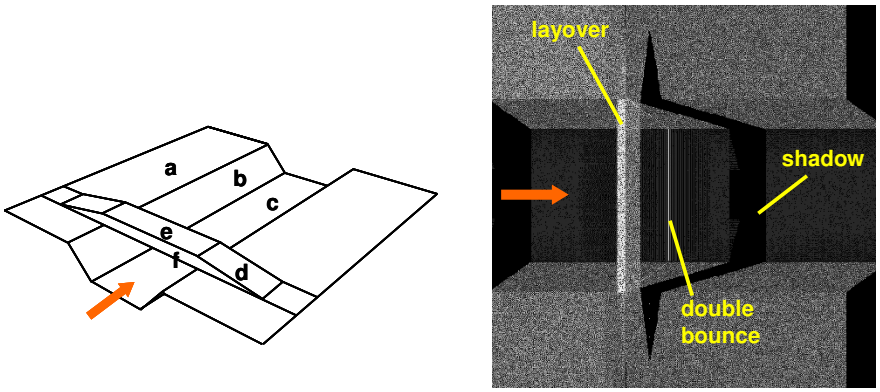

Figure 6: Bridge model used for simulations (left). Terrain (a), Sides of valley (b), valley basement (c), bridge ramp (d), bridge deck (e), bridge side (f). Simulation result (right). Illumination direction marked with arrow

The bridge model used for simulation is shown in Figure 6 (left). The model describes a simple bridge over a valley. In a first simulation, 'water' was chosen as material for valley basement (plane c), 'vegetation' for the valley sides and the rest of the ground. The bridge body's (planes d,e,f) reflection was modelled to be a mixture of direct and Lambertian type (50% each). A visualization of the simulation result is shown in Figure 6 (right). A layover area is clearly visible, caused by signal contribution from bridge deck and side. Part of the signal energy reaching the bridge side is reflected to the water and from there back to the sensor and vice-versa, respectively (double-bounce). This simulation result will be starting point for further investigations with more complex models where sub- and superstructures will be added, resulting in multi-bounce reflections. These additionally structures will also allow investigations concerning influence of different aspect angles.

RESULTS AND CONCLUSION

The segmentation approach using initially stored parameters was applied to several RADARSAT-1 images of Norway. They include two suspension bridges and have a resolution of approx. 9 m. The images were recorded at different seasons and also under slightly different incidence angles, but all from ascending orbit. The height was derived from the distance of segmented parallel lines, and results are presented in Table 1. For the first bridge (Askoy) the mean height was derived from eight images, for the second bridge (Osteroy) from five images.

Table 1: Derived mean height from RADARSAT-1 images .

Bridge	Ground Truth	Derived Mean Height
Askoy	62 m	58 m
Osteroy	53 m	54 m

The segmentation of the parallel lines based on the initially stored parameters failed only for one of the given nine images of the Askoy-bridge. The derived heights are promising, keeping in mind the rather coarse resolution of only approx. 9 m.

No time series was available for the bridge shown in Figure 3. The segmentation was therefore applied only to one high resolution airborne image, and the result is presented in Table 2.

Table 2: Derived height from AeS-1 image .

Bridge	Ground Truth	Derived Height
Dorsten	10.8 m	9 m

ISBN 978-3-925143-79-3

This result is almost 2 m lower than the ground truth, but as ground truth only a LIDAR-DEM was available. Additionally the splitting of the first signal due to the railing has probably some influence on the result. But nevertheless, the feature ‘parallel lines’ was also detectable.

Based on these results it can be derived that the feature 'parallel lines' is a reliable one for change detection, where the first line of the pair is expected to be located at closest distance to the sensor. This simple bridge model should be enhanced to describe bridges in more detail and make the approach more flexible concerning reliable imaging constellations. In future work, the impact of varying weather conditions to the feature extraction should be analyzed. The simulator tool will be enhanced, so that more different materials and more complex bridge models can be used for the initial parameter and constraints estimation, respectively. Finally more different bridge objects should be used for verification of the approach.

ACKNOWLEDGEMENTS

We want to thank Dr. Med. Mario Iasevoli for providing the photos of the bridges in Dorsten.

REFERENCES

ii Documentation: http://www.dlr.de/tsx/documentation/EUSAR-TX-Mission.pdf . Website: http://www.dlr.de/tsx/start_en.htm

ii Documentation: http://www.radarsat2.info/about/v2-6pager_marketing_6pg-web.pdf . Website: http://www.radarsat2.info/

iii Documentation: http://www.telespazio.it/pdf/Brochure_cosmo_eng_0607.pdf . Website: http://www.telespazio.it/cosmo.html

iv Inglada J, Mercier G, 2006. The multiscale change profile: a statistical similarity measure for change detection in multitemporal SAR images. In: Proc. of IGARSS, CD, 4p

v Matsouka M, Yamazaki F, 2004. Building damage detection using satellite SAR intensity images for the 2003 Algeria and Iran earthquakes. In: Proc. of IGARSS, CD, 4p

vi Bach H, Appel F, Fellah K, de Fraipont P, 2005. Application of flood monitoring from satellite for insurances. In: Proc. of IGARSS, CD, 4p

vii Soergel U, 2003. Iterative Verfahren zur Detektion und Rekonstruktion von Gebäuden in SAR- und InSAR-Daten. Dissertation.

viii Soergel U, Thoenessen U, Brenner A, Stilla U, 2006. High resolution SAR data: new opportunities and challenges for the analysis of urban areas. In: IEE Proceedings - Radar, Sonar, Navigation, 153(3):294-300

ix Tupin F, Maitre H, Mangin J-F, Nicolas J-M, Pechersky E, 1998. Detection of linear features in SAR images: application to road network extraction. IEEE Transactions on Geoscience and Remote Sensing, 36(2): 434-453

x Gamba P., Houshmand B, Saccani M, 2000. Detection and extraction of buildings from interferometric SAR data. IEEE Transactions on Geoscience and Remote Sensing, 38(1): 611-617

xi Thiele A., Cadario E, Schulz K, Thoennessen U, Soergel U, 2007. Detection and extraction of buildings from interferometric SAR data. IEEE Transactions on Geoscience and Remote Sensing, , 45 (11), Part 1:. 3583-3593

xii Wang Y, Zheng Q, 1998. Recognition of roads and bridges in SAR images. Pattern Recognition, 31(7): 953-962

xiii Soergel U, Cadario E, Gross H, Thiele A, Thoennessen U, 2006. Bridge detection in multi-aspect high-resolution interferometric SAR data. In: Proc. of 6th European conference on synthetic aperture radar, EUSAR 2006, CD, 4p

xiv Raney R K, 1983. The Canadian SAR Experience. In: Satellite Microwave Remote Sensing, edited by T.D. Allan, Ellis Horwood Ltd., Chichester, Chapter 13: 223-234 (see also: http://ccrs.nrcan.gc.ca/radar/ana/confed_e.php)

xv Raney R K, 1998. Radar Fundamentals: Technical Perspective. In: Henderson, Floyd M., and Anthony J. Lewis, ed. Manual of Remote Sensing 3rd Edition: Principles and Applications of Imaging Radar, American Society for Photogr. and Rem. Sensing, 2: 9-130

xvi Robalo J, Lichtenegger J, 1999. ERS-SAR Images a bridge. Earth Oberservation Quarterly, ESA, 7-10 (see also: http://esapub.esrin.esa.it/eoq/eoq64/bridge.pdf)

xvii Lee J-S, Ainsworth T L, Krogagor E, Boerner W-M, 2006. Polarimetric analysis of radar signature of a manmade structure. Proc. of IGARSS, CD, 4p

xviii Loh K, Shinozuka M, Mansouri B, Ghanem R, 2004. Structural Damage Detection and Identification Using Synthetic Aperture Radar. The 17th ASCE Engineering Mechanics Conference, University of Delaware, June 13-16

xix Schwaebisch M, Moreira J, 1999. The high resolution airborne interferometric SAR AeS-1. In: Proceedings of the Fourth International Air-borne Remote Sensing Conference and Exhibition, 540-547

xx Soergel U, Gross H, Thiele A, Thoennessen U, 2006. Extraction of Bridges over Water in Multi-Aspect High-Resolution InSAR Data. In: Proceedings PCV, W. Förstner, R. Steffen (eds.), September 2006, Bonn, 36(3):185-190

xxi Steger C, 1998. An Unbiased Detector of Curvilinear Structures. IEEE Trans. Pattern Analysis Machine Intelligence, 20(2):113-125

xxii Ulaby F T, Moore R K, Fung A K, 1981-1986. Microwave Remote Sensing: Active and Passive. Vols. 1-3, Artech House

ISBN 978-3-925143-79-3